Analysis of Tumor Cell Evolution in a Melanoma: Evidence of Mutational and Selective Pressure for Loss of *p16^{ink4}* and for Microsatellite Instability

Albert Rübben, Philipp Babilas, Jens M. Baron, Anja Hofheinz, Mark Neis, Florian Sels, and Markus Sporkert

Department of Dermatology, University Hospital of the RWTH Aachen, Germany

Tumorigenesis and tumor progression can be considered an evolutionary process. In order to deduce information on the mutational and selective pressures during melanoma progression we performed microsatellite analysis at 42 autosomal and two X-linked loci in a microdissected primary melanoma and its nine metastases. Loss of heterozygosity at locus D9S259 was the only genetic change observed in all metastases. The pattern of loss of heterozygosity at loci D9S162 and D9S171 within the region of common loss on chromosome 9p21 which encompasses the tumor suppressor gene *p16^{ink4}* enabled the distinction of four genetically different tumor cell populations. Three cell lineages showed homozygous loss of the *p16^{ink4}* gene, which evolved independently in each tumor cell population within the primary tumor. Additional allele losses could be demonstrated at markers D14S53 and DXS998. The fourth lineage did not demonstrate loss of heterozygosity at loci D9S162 and D9S171 and contained the wild type *p16^{ink4}* gene but was characterized by abundant microsatellite instability. The evolutionary approach towards tumorigenesis and tumor progression used in this study thus confirms the role of *p16^{ink4}* inactivation for melanoma progression but not for melanoma initiation; it suggests the existence of additional putative tumor suppressor genes located on 9p as well as on the long arm of chromosome 14 and shows that microsatellite instability may represent an alternative pathway of tumor cell evolution in malignant melanoma. ***Key words: microdissection/ SSCP analysis. J Invest Dermatol 114:14–20, 2000***

Tumorigenesis and tumor progression can be considered an evolutionary process in which mutant and more tumorigenic subpopulations are sequentially selected and derived from less tumorigenic or benign progenitor cells (Nowell, 1976). Many human tumors are the result of a set of multiple mutations (Loeb and Christians, 1996) which seem to be specific for the affected tissue and tumor entity. The sequence of the required mutations is known only for a few cancers such as colon cancer (Fearon and Vogelstein, 1990; Boland *et al*, 1995) but for most other human malignant tumors the exact number and nature of mutations has still to be determined.

The main focus of current research is the identification and description of mutations and the analysis of the mutation rate during the process of malignant conversion and progression. Less attention is directed towards the other determinants of tumor cell evolution such as the degree of the selective pressure, the fitness of the selected tumor cells (Tomlinson and Bodmer, 1999), and the exact number of possible genetic pathways during tumor progression. Knowledge of the main factors determining the evolutionary process in malignant tumors could be used to predict disease progression in individual patients and to evaluate the effects of specific treatment modalities that alter the selective and mutational pressures in the tumor microenvironment.

Genetic heterogeneity within the primary tumor is indirect evidence of the mutational and selective pressures during tumorigenesis and early steps of tumor progression whereas heterogeneity between the primary tumor and its metastases elucidates the processes during later steps of malignant progression. Genetic heterogeneity reflects the multistep nature of the neoplastic transformation and it can be observed in many human malignancies (Shibata *et al*, 1992, 1993; Mirchandani *et al*, 1995; Fujii *et al*, 1996; Tollenaar *et al*, 1997) as well as in malignant melanoma (Wiltshire *et al*, 1995; Boni *et al*, 1998; Morita *et al*, 1998).

Information concerning the possible pathways of tumor cell evolution can be obtained by generating a genealogic tree based on genetic markers (Dracopoli *et al*, 1987). In a recent study, this approach has been refined by analyzing colon cancers with mismatch repair deficiency (Tsao *et al*, 1999). Mismatch repair deficiency leads to multiple mutations within repetitive microsatellite DNA. These mutations can be utilized as a molecular clock of tumor cell evolution because the noncoding microsatellite DNA does not underlie a selective pressure. It is thereby possible not only to identify individual tumor cell populations but also to determine the phylogenetic distance between individual tumor cell clones during the process of tumor cell evolution.

Manuscript received March 9, 1999; revised September 17, 1999; accepted for publication September 20, 1999.

Reprint requests to: Priv.-Doz. Dr. A. Rübben, Hautklinik, Universitätsklinikum der RWTH Aachen, Pauwelsstraße 30, 52074 Aachen, Germany. Email: Albert.Ruebben@post.rwth-aachen.de

Abbreviations: CA, cytosine-adenosine; cdk, cyclin-dependent kinase; LOH, loss of heterozygosity; pRb, retinoblastoma protein; TG-SSCP, temperature-gradient single strand conformation polymorphism.

In this study we took a similar approach in order to describe the evolutionary process in a malignant melanoma. The predominating form of genetic instability in malignant melanoma seems to be the occurrence of structural mutations and especially of large deletions rather than mismatch repair deficiency (Healy *et al*, 1996; Ohta *et al*, 1996; Morita *et al*, 1998; Wagner *et al*, 1998). We hypothesized that genetic instability within melanoma cells should lead to a gradual increase in the amount of random DNA deletions during the process of melanoma progression. DNA deletions can be demonstrated by loss of heterozygosity (LOH) at microsatellite DNA loci using the polymerase chain reaction (Boland *et al*, 1995). LOH is a robust marker for distinguishing individual tumor cell populations but only nonselected mutations can be used to calibrate a molecular clock of tumor progression. It is not known a priori which deletions target a tumor suppressor gene and are thus selected and which mutations evolve without selection. In this study we have therefore determined LOH at multiple and randomly distributed microsatellite loci in an advanced but slowly progressing melanoma. We assumed that in this particular case the tumor cells should have had enough time to accumulate a sufficient amount of selected as well as nonselected structural mutations during tumor progression, which could be utilized to measure the degree of genetic instability during tumor progression, to determine the amount of genetic heterogeneity in the primary as well as in metastases, to establish a genealogic tree reflecting tumor cell evolution in the analysed patient, and to estimate the phylogenetic distance between genetically different tumor cell populations.

MATERIALS AND METHODS

Patient and analysed tumor specimens In 1987 a large nodular melanoma approximately 3 cm in diameter with a vertical thickness of 15 mm which already showed a satellite metastasis at its margin was removed from the right forearm of a 46-y-old female patient. Within 8 y, the patient developed eight cutaneous metastases at the right arm, three axillary lymph node metastases and one gastric metastasis which led to the death of the patient. We were able to analyse tissue of the primary tumor, the satellite metastasis, four of the eight cutaneous metastases as well as the lymph node and gastric metastases by microsatellite polymerase chain reaction (PCR).

Microdissection and DNA extraction DNA was extracted from formalin-fixed paraffin-embedded tissue specimens. DNA from the metastases was obtained from 10 consecutive tissue sections 10 μm thick while DNA from the primary tumor was extracted after microdissection. Microdissection was performed on 10 μm thick deparaffinized tissue sections using adhesive for picking of the cells as previously described (Turbett *et al*, 1996). With this technique we isolated regions of interests containing approximately 5000–10000 malignant cells. The specimens were digested with proteinase K and the DNA was eluted using the Qiagamp Tissue Kit (Quiagen, Hilden, Germany) according to the manufacturer's recommendations. DNA obtained from metastases was eluted in 100 μl of $H_2O_{dest.}$ and DNA obtained from microdissected areas was eluted in 50 μl of H_2O_{dest}.

Microsatellite analysis DNA from the metastases was analysed at 44 microsatellite loci which were chosen in order to analyse the region of common loss in melanoma on the short arm of chromosome 9 in detail as well as to screen the genome for loss of heterozygosity at random (**Table I**). DNA from the microdissected primary tumor was analysed only for specific allele losses. PCR with unlabeled microsatellite primers (Research Genetics, Huntsville, AL) or with primers labeled 5′ with digoxigenin (Genset, Paris, France) was performed using a final primer concentration of 1.5 μM. PCR was done in a total volume of 50 μl with 2.5 U of the Taq-polymerase AmpliTaq Gold (Perkin Elmer, Roche Diagnostics, Basel, Switzerland) according to the manufacturer's recommendations (35 cycles: 1 min 55°C, 1 min 72°C, 1 min 94°C) using the DNA Thermal Cycler 480 (Perkin Elmer). PCR with DNA from metastases was performed using 1–2 μl of the DNA solution whereas PCR with DNA from microdissected areas needed 2–5 μl of DNA solution for each assay.

PCR products were analysed in three different ways. All samples were first screened by temperature-gradient single strand conformation polymorphism (TG-SSCP) analysis. This technique allows the demonstration of LOH as well as the visualization of mutations within the amplified repetitive DNA caused by microsatellite instability. TG-SSCP analysis was performed as previously described (Rübben *et al*, 1995). Briefly, 3.5 μl of each PCR product were mixed with a stop solution containing 3 μl of 95% formamide, 10 mM NaOH, 0.05% bromophenol blue and 0.05% xylene cyanol. The mixture was denatured at 100°C for 5 min, rapidly chilled on ice for 3 min and then filled in a single well of a horizontal electrophoresis gel. Electrophoresis with a linear temperature gradient from the cathode to the anode ranging from 19°C to 23°C was performed in a 0.5% Hydrolink gel matrix (AT Biochem, Malvern, PA) at 300 V for 3.5 h using a commercially available temperature-gradient horizontal gel electrophoresis device (DIAGEN TGGE System, Hilden, Germany). Nucleic acids were visualized by silver staining. At least two independent PCR assays and two TG-SSCP analyses were perfomed with each sample showing LOH in order to rule out PCR or TG-SSCP artefacts. An additional independent PCR was performed with one primer labeled 5′ with digoxigenin in order to confirm LOH in these samples by conventional sequencing gel analysis. These PCR products were directly blotted onto a nylon membrane during electrophoresis using the GATC 1500 direct blotting sequencer (GATC, Konstanz, Germany). Bands were visualized after incubation of the membranes with an antidigoxigenin antibody (Boehringer, Mannheim, Germany) conjugated to horseradish peroxidase using the enhanced chemoluminescence system (ECL detection system, Amersham Pharmacia, Uppsala, Sweden). Chemoluminescence was recorded on X-ray films (Kodak T-mat-G). The same membranes were further hybridized with a fluorescein-labeled $(CA)_{10}$-oligonucleotide (Genset) in order to exclude PCR artefacts which easily accumulate during PCR from formalin-fixed tissue specimens. Hybridization was performed under stringent conditions (5 × SSC, 0.1% SDS) for 4 h at 50°C. After washing (1 × SSC, 0.1% SDS, 50°C, 15 min), hybridization was demonstrated with an antifluorescein antibody conjugated to horseradish peroxidase.

Mutation analysis of the *p16^{ink4}* gene Exon 1 of the *p16^{ink4}* gene was amplified by PCR with the primer pair: 5′AGCAGCATGGAG-CCTTCGG3′, 5′CTACCCACCTGGATCGGC3′, which gives rise to a product of 141 bp length. Annealing temperature was 60°C. Exon 2 was amplified in two overlapping fragments of 182 bp and 194 bp length using the following primer pairs: 5′TGGCAGGTCATGATGATGGGG3′, 5′GCATCGCGCACGTCCAGC3′, and 5′GGACACGCTGGTGGT-GCT3′, 5′TCCTCACCTGAGGGACCT3′. The annealing temperatures used were 60°C and 58°C and the primer concentration was 1.5 μM. PCR was performed with 35 cycles in a total volume of 50 μl with 2.5 U of the Taq-polymerase AmpliTaq Gold according to the manufacturer's recommendations and the PCR products were analysed by TG-SSCP analysis as described before.

Analysis of homozygous loss of the *p16^{ink4}* gene Competitive multiplex PCR was performed in order to demonstrate homozygous loss of the *p16^{ink4}* gene. The 194 bp product of exon 2 was coamplified with part of the *β-actin* gene. For amplification of exon 3 of the *β–actin* gene we used the primer pair XAHR20, XAHR17 (Research Genetics) which gives rise to a 289 bp product. The final primer concentration was 1.5 μM. In order to amplify PCR products of equal quantity, the ratio between the primers for the *β–actin* gene and the *p16^{ink4}* gene was adapted to 3:1 (**Fig 1*a***). PCR was performed with 35 cycles using an annealing temperature of 58°C.

RESULTS

Microsatellite analysis of the metastases The metastases of the patient were screened by TG-SSCP analysis for LOH and for microsatellite instability at 44 microsatellite loci. LOH was confirmed by analysis in a conventional sequencing gel. Specificity of the amplified DNA was further probed by Southern blot hybridization with a $(CA)_{10}$-oligonucleotide.

Figure 2 exemplifies the methods used. TG-SSCP analysis of microsatellite D9S162 produced four partly overlapping bands (**Fig 2*a***) which corresponded to the two alleles of different molecular size (**Fig 2*b***). The microsatellite locus D9S162 was heterozygous in DNA obtained from normal formalin-fixed paraffin-embedded tissue (N1, N2) of the patient. LOH of the allele of higher molecular size was found in metastasis M1, whereas the smaller allele was lost in metastasis M2.

Figure 2(*b*) shows that alleles of lower molecular size were amplified with higher efficiency by the PCR process in some cases (N2). The degree of this bias seemed to vary depending on the quality of the DNA originating from formalin-fixed tissue (N1 *versus* N2).

Table I. Genotypes of melanoma metastases determined at 44 microsatellite loci[a]

		primary			metastases								
no.		P1	P2	P3	M1	M2	M3	M4	M5	M6	M7	M8	M9
month/year			5/87		5/87	5/90	10/90	10/90	11/90	12/91	12/94	12/94	6/95
localisation (right arm)			forearm		forearm	upper arm	forearm	upper arm	forearm	axilla	axilla	axilla	stomach
microsatellite	chromosomal localization	alleles											
D1S187	1p22	ND	ND	ND	NP	○/○	○/○	○/○	○/○	●/○	○/○	○/○	ND
CD8A	2p12	ND	ND	ND	NP	○/○	○/○	○/○	○/○	●/○	○/○	○/○	ND
D2S211	2q34-q37	ND	ND	ND	NP	○	○	○	○	I	○	○	ND
HOX7	4p16.1	ND	ND	ND	NP	○	○	○	○	○	○	○	ND
D4S171	4p13-p11	ND	ND	ND	NP	○	○	○	○	○	○	○	ND
D4S192	4q27-q31	ND	ND	ND	NP	○/○	○/○	○/○	○/○	I/○	○/○	○/○	ND
D5S350	5p13-p14	ND	ND	ND	NP	○	○	○	○	○	○	○	ND
D5S107	5q11-q13	ND	ND	ND	NP	○/○	○/○	○/○	○/○	●/I	○/○	○/○	ND
D6S105	6p21.3	ND	ND	ND	NP	○	○	○	○	I	○	○	ND
D6S297	6q27	ND	ND	ND	○	○	○	○	○	I	○	○	ND
D7S547	7p21-p13	ND	ND	ND	○/○	○/○	○/○	○/○	○/○	●/I	○/○	○/○	ND
EGFR	7p12-q11	ND	ND	ND	○	○	○	○	○	I	○	○	ND
LPL	8p22	ND	ND	ND	○	○	○	○	○	○	○	○	ND
D8S85	8q21-q22	ND	ND	ND	○	○	○	○	○	○	○	○	ND
D9S162	9p22-p21	○/●	○/○	●/○	●/○	○/●	●/○	○/●	○/●	○/○	I/●	○/●	○/●
D9S171	9p21	○/●	●/○	●/○	●/○	○/●	●/○	○/●	○/●	○/I	○/●	○/●	○/●
D9S126	9p21	ND	ND	ND	○	○	○	○	○	○	○	○	○
D9S265	9p21	ND	ND	ND	○	○	○	○	○	○	○	○	○
D9S259	9p21	●/○	●/○	●/○	●/○	●/I	●/○	●/○	●/○	●/○	●/I	●/○	●/○
D9S270	9p21	ND	ND	ND	●/○	●/○	●/○	●/○	NP	I/○	●/○	●/○	ND
D10S169	10q26-qter	ND	ND	ND	○/○	○/○	○/○	○/○	○/○	●/○	○/○	○/○	ND
FGF3	11q13	ND	ND	ND	○	○	○	○	○	I	○	○	ND
D11S29	11q23.3	ND	ND	ND	○/○	○/○	○/○	○/○	○/○	NP	○/○	○/○	ND
D12S61	12	ND	ND	ND	○/○	○/○	○/○	○/○	○/○	●/○	○/○	○/○	ND
D13S139	13q12-q14	ND	ND	ND	○/○	○/○	○/○	○/○	○/○	○/○	○/○	○/○	ND
D13S159	13q32	ND	ND	ND	○/○	○/○	○/○	○/○	○/○	○/I	○/○	○/○	ND
D14S53	14q24.3-q31	●/○	○/●	○/●	○/●	●/○	○/●	●/○	●/○	○/○	●/○	●/○	ND
D15S519	15	ND	ND	ND	○/○	○/○	○/○	○/○	○/○	○/I	○/○	○/○	ND
D15S59	15q14-qter	ND	ND	ND	○/○	○/○	○/○	○/○	○/○	○/○	○/○	○/○	ND
D15S107	15q26	ND	ND	ND	○/○	○/○	○/○	○/○	○/○	●/○	○/○	○/○	ND
D17S1176	17p13.1	ND	ND	ND	○	○	○	○	○	I	○	○	ND
D17S520	17p12	ND	ND	ND	○	○	○	○	○	I	○	○	ND
HOX2B	17q21-q22	ND	ND	ND	○/○	○/○	○/○	○/○	○/○	○/○	○/○	○/○	ND
D18S40	18p11.21	ND	ND	ND	○/○	○/○	○/○	○/○	○/○	○/I	○/○	○/○	ND
D18S42	18q21.2-q21.3	ND	ND	ND	○	○	○	○	○	I	I	○	ND
D19S49	19q12-q13.1	ND	ND	ND	○	○	○	○	○	I	○	○	ND
KLK	19q13.3-q13.4	ND	ND	ND	○/○	○/○	○/○	○/○	○/○	●/○	○/○	○/○	ND
D20S27	20p12	ND	ND	ND	○/○	○/○	○/○	○/○	○/○	○/○	○/○	○/○	ND
SRC	20q11.2	ND	ND	ND	NP	○	○	○	○	○	○	○	ND
D21S258	21q11	ND	ND	ND	○/○	○/○	○/○	○/○	○/○	I/I	○/○	NP	ND
IL2RB	22q12	ND	ND	ND	○/○	○/○	○/○	○/○	○/○	I/○	○/○	NP	ND
D22S294	22q13.1-qter	ND	ND	ND	○	○	○	○	○	○	○	NP	ND
DXS984	xq25-q26	ND	ND	ND	○	○	○	○	○	○	○	○	○
DXS998	xq27	●/○	○/○	●/○	●/○	●/○	●/○	●/○	●/○	I/○	●/○	●/○	●/○
LOH/informative chromosome arms:		ND	ND	ND	3/15	3/19	3/19	3/19	3/19	9/18	3/19	3/17	ND
microsatellite instability/ tested loci:		ND	ND	ND	0/34	1/44	0/44	0/44	0/43	20/43	3/44	0/41	ND

[a]Alleles: ○/○, heterozygous; ○, noninformative; ○/●, loss of allele of lower molecular size; ●/○, loss of allele of higher molecular size; I, mutated allele (microsatellite instability); NP, no PCR-product; ND, not done.

Microsatellite instability could be visualized by both techniques. The band shift demonstrated by TG-SSCP analysis with microsatellite D9S171 in metastasis M6 (**Fig 2*a***) corresponds to a mutant allele of lower molecular weight in the sequencing gel (**Fig 2*b***).

In some samples, PCR amplification from formalin-fixed tissue yielded nonspecific bands within the range of the expected microsatellite DNA as demonstrated by Southern blot hybridization (**Fig 2*c***). Interpretation of TG-SSCP analysis was less disturbed by these nonspecific PCR products as the band pattern generated by TG-SSCP reflects the DNA sequence. On the other hand, interpretation of TG-SSCP band patterns requires some practice as single strand DNA molecules may adopt unstable conformations during electrophoresis, which may then mimic a band shift.

Table I summarizes the microsatellite data of all metastases. About half of the tested loci were informative for LOH analysis. Metastases M1–M5 and M7–M9 demonstrated a pattern of LOH restricted to the region of common loss on chromosome 9p as well as on two additional loci at D14S53 (14q24.3-q31) and DXS998 (Xq27). In contrast, metastasis M6 showed multiple LOH as well as microsatellite instability at different loci scattered on various

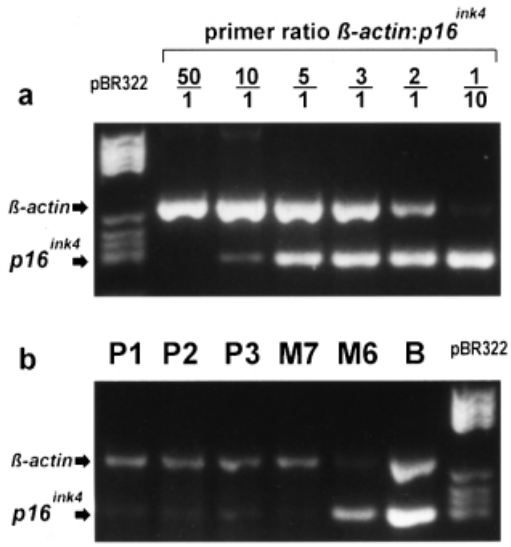

Figure 1. Competitive multiplex PCR for demonstration of loss of the *p16*^{ink4} gene. (*a*) Calibration of primer ratio, (*b*) PCR with extracted DNA from primary tumor (P1–P3), metastases (M6, M7) and blood of the patient. pBR322, molecular size marker.

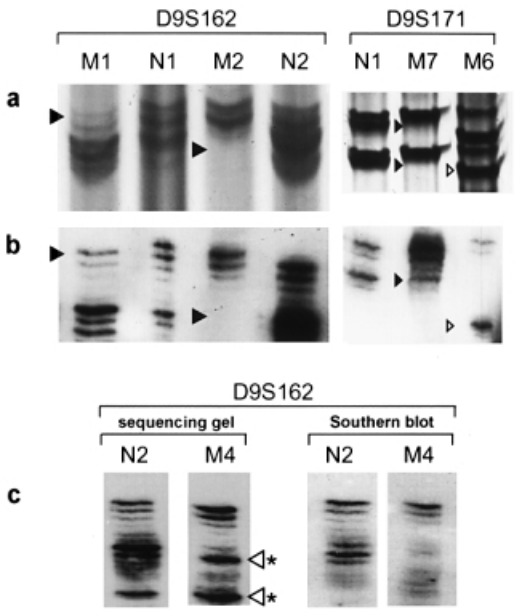

Figure 2. Comparison of the methods used for the analysis of PCR-amplified microsatellite DNA. (*a*) TG-SSCP analysis, (*b*) analysis in a sequencing gel, (*c*) conventional sequencing gel *versus* Southern blot hybridization of the blotted sequencing gel with a $(CA)_{10}$-oligonucleotide; M, metastases; N, normal formalin-fixed tissue specimens; ▶ loss of DNA bands (LOH); ▷ mutated DNA bands (microsatellite instability); ◁* points to nonspecific DNA bands.

chromosomes. The degree of genetic instability was highest in metastasis M6 with LOH on nine of 18 chromosome arms harbouring informative microsatellite loci and microsatellite instability at 20 of 43 analysed markers. Microsatellite instability in M6 was confirmed by hybridization with the $(CA)_{10}$ probe. The other metastases showed significantly lower genetic instability with LOH at three of 15–19 chromosome arms harboring informative microsatellite loci and microsatellite instability at 0–3 of 44 tested markers.

The pattern of LOH at loci D9S162 and D9S171 within the region of common loss on chromosome 9p which encompasses the

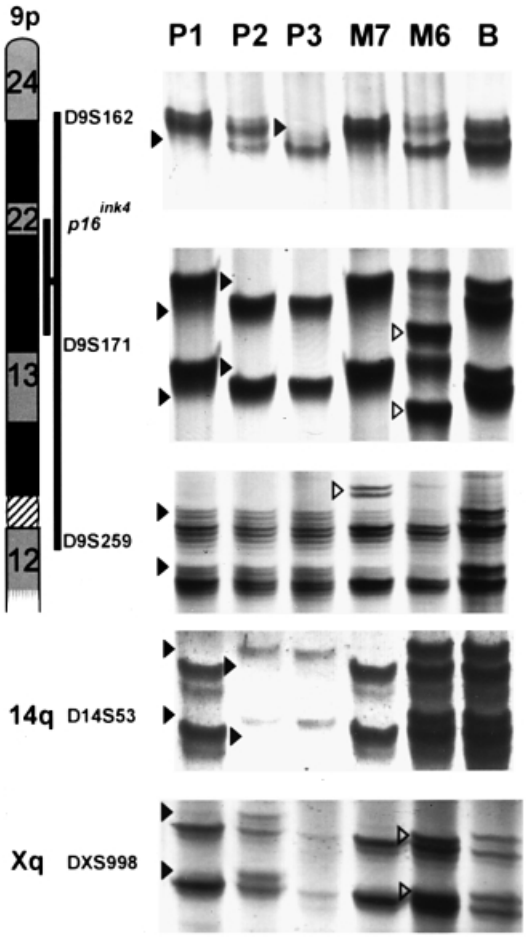

Figure 3. Characterization of tumor cell populations. TG-SSCP analysis of PCR-amplified microsatellite DNA obtained from microdissected tissue of the primary tumor (P1–3), from metastases (M7, M6) and from the patient's blood (B). ▶ loss of DNA bands (LOH); ▷ mutated DNA bands.

tumor suppressor gene *p16*^{ink4} enabled the distinction of three genetically different tumor cell populations in the metastases. Tumor cells in metastases M1 and M3 differed from tumor cells in metastases M2, M4–M5, M7–M9 by the loss of the opposite alleles at two microsatellite loci (**Table I**, **Fig 2**). In contrast, cells of metastasis M6 did not harbour LOH in this region but displayed microsatellite instability at D9S171 (**Fig 2** and **Fig 3**). LOH at locus D9S259 was the only genetic change observed in all metastases.

Microsatellite analysis of the primary tumor Microallelotyping of the primary tumor was performed in order to distinguish whether the observed genetic heterogeneity evolved within the primary tumor or in the metastases. Fifteen different microdissected regions of the primary nodular melanoma were analysed for LOH at microsatellite loci D9S162, D9S171, D9S259, DX998, and D14S53. Three regions (P1–P3) of the primary tumor revealed tumor cell populations of different genotypes (**Table I**, **Fig 3**).

Analysis of the *p16*^{ink4} gene LOH in the region of common loss on chromosome 9p suggested heterozygous or homozygous loss of the *p16*^{ink4} tumor suppressor gene. The status of the *p16*^{ink4} gene in the microdissected cell populations of the primary tumor as well as in the metastases was analysed by competitive multiplex PCR. As previously shown in **Fig 2**, the low quality of DNA from formalin-fixed tissue could lead to overamplification of the smaller PCR product during multiplex PCR. Therefore, the PCR product of the *p16*^{ink4} gene was chosen to be smaller in size than the control gene *β-actin* in order to prevent that the low quality of DNA could mimic loss of *p16*^{ink4}. Homozygous loss of the *p16*^{ink4} gene could be

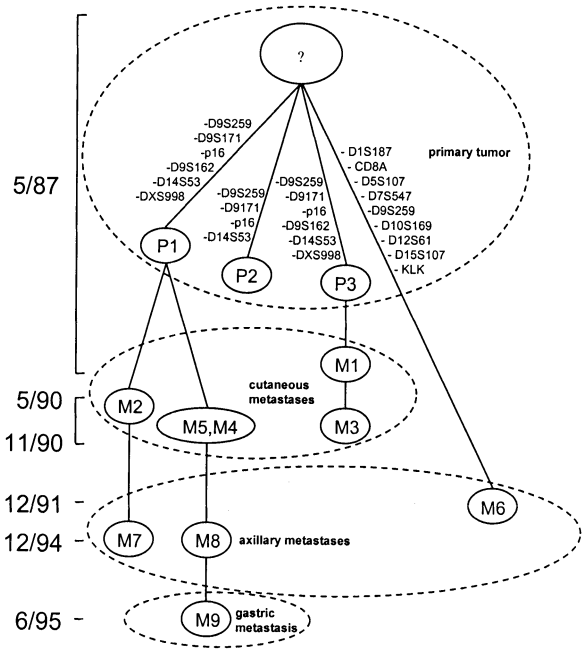

Figure 4. Putative genealogic tree of tumor cell evolution in the analysed patient obtained from data summarized in Table I.

demonstrated in three regions of the primary tumor (P1-P3) as well as in all metastases which also displayed LOH at the loci D9S162 and D9S171 (**Fig 1*b***). No loss of the *p16^{ink4}* gene could be detected in metastasis M6. The weak amplification of the *β-actin* gene was due to the reduced quality of the eluted DNA from this metastasis. TG-SSCP analysis of exons 1 and 2 of the *p16^{ink4}* gene was performed with DNA from metastasis M6 but did not demonstrate a mutation within the analysed coding sequences, which might have constituted an alternative mechanism of *p16^{ink4}* inactivation.

DISCUSSION

The aim of this study was to gain information on the mutational and selective pressures during melanoma progression by the analysis of LOH at multiple genetic loci in one primary melanoma and its nine metastases. The pattern of LOH at different microsatellite loci found in microdissected tissue specimens of the primary tumor and in the metastases revealed a high degree of genetic heterogeneity in the tumor.

These data allow the construction of a simple phylogenetic tree of tumor cell evolution in the analysed patient in analogy to the evolutionary tree describing species radiation (**Fig 4**): Assuming a monoclonal origin of malignant melanoma the data indicate early segregation of tumor cell populations within the primary tumor into four different lineages, three demonstrating homozygous loss of the *p16^{ink4}* gene and the fourth characterized by microsatellite instability leading to metastasis M6. Tumor cells with homozygous loss of the *p16^{ink4}* gene can be subdivided into three independent tumor cell clones (P1, P2, P3) by the pattern of LOH on chromosome 9p. Metastasis M7 seems to originate from M2 as both shared microsatellite instability at D9S259. M4, M5, M8, and M9 seem to represent one lineage as they did not share any detectable microsatellite instability at this locus. It is interesting to note that the metachronous cutaneous and axillary metastases originated from different tumor cell clones in the primary tumor.

The initial hypothesis of our study was that genetic instability within melanoma cells should lead to a gradual increase in the amount of random and nonselected DNA deletions during the process of melanoma progression, which could then be utilized to calibrate a molecular clock of tumor cell evolution. This assumption could not be verified in our study as we found extensive genetic heterogeneity within tumor cell populations of the primary tumor but only very few additional structural mutations in the resulting metastases. For the same reason it was not possible to use the genetic data obtained by LOH analysis for an exact measurement of the degree of genetic instability during tumor progression and for assessment of the phylogenetic distance between genetically different tumor cell populations.

Nevertheless, the tumor cell genealogy presented allows us to draw preliminary conclusions about important aspects of tumorigenesis and tumor cell evolution in malignant melanoma.

The tumor suppressor gene *p16^{ink4}* (CDKN2/MTS1) located on the short arm of human chromosome 9 plays a key role in cell cycle control. It binds to the cyclin-dependent kinase 4 enzyme and thus inhibits its ability to phosphorylate substrates that enable the transit through the G_1 phase. *p16^{ink4}* is frequently deleted in melanoma cell lines and is found to be mutated in a subset of families with hereditary malignant melanoma (Kamb *et al*, 1994; Goldstein and Tucker, 1997). It is therefore believed to represent a primary genetic target in melanoma tumorigenesis. In the analysed tumor, three unrelated and independent chromosomal rearrangements resulted in homozygous loss of *p16^{ink4}* and led to distinct tumor cell clones which otherwise appeared to be genetically rather stable. This is indicative of a high selective pressure for loss of *p16^{ink4}* in the tumor microenvironment and it underlines the importance of *p16^{ink4}* inactivation for melanoma progression. The recent work of Morita *et al* (1998) showed a similar picture of melanoma evolution. By analysing genetic profiles in primary melanomas and their metastases they could identify a melanoma which also displayed two distinct tumor cell populations showing allele loss at opposing loci on 9p. Although loss of *p16^{ink4}* is believed to represent a common and important step in melanoma progression and seems to be strongly selected in the analysed tumor, it is not present in all cases of advanced malignant melanoma (Glendening *et al*, 1995; Healy *et al*, 1996; Wagner *et al*, 1998). This apparent inconsistency may in part be explained by the concept of regulatory pathways targeted as functional units during tumorigenesis. It has been demonstrated that mutations of *pRb* or *cdk4* have the same effect on cell cycle control and substitute for loss of function of *p16^{ink4}* in melanoma cell lines (Bartkova *et al*, 1996), and it has been assumed that the *p16^{ink4}*-cyclin D/*cdk4-pRb* pathway is altered in the majority of melanoma cases.

Controversy has arisen about the timepoint of *p16^{ink4}* inactivation during melanoma tumorigenesis. The finding of *p16^{ink4}* mutations in about one fourth of all kindreds with familial malignant melanoma and the demonstration of *p16^{ink4}* mutations in dysplastic nevi has indicated that loss of *p16^{ink4}* function might represent an initiating event in melanoma tumorigenesis (Walker *et al*, 1995; Goldstein and Tucker, 1997; Lee *et al*, 1997). On the other hand, analysis of expression of *p16^{ink4}* in melanomas at different stages has shown that loss of *p16^{ink4}* function is mainly restricted to invasive and metastatic tumors and does not seem to be required for tumor initiation (Reed *et al*, 1995; Talve *et al*, 1997). Moreover, in sporadic malignant melanoma, the predominant type of mutation leading to *p16^{ink4}* inactivation seems to be homozygous loss rather than point mutation (Healy *et al*, 1996; Ohta *et al*, 1996; Morita *et al*, 1998; Wagner *et al*, 1998). The occurrence of homozygous loss fits better to the concept of a secondary genetic change taking place in an already genetically unstable malignant cell clone. Our data support this assumption as loss of the *p16^{ink4}* gene evolved in the analysed tumor independently in three distinct malignant cell clones and must therefore represent a genetic event that arose after the initial clonal expansion. As our study only focuses on one single tumor, we cannot rule out that in a different genetic setting and especially in patients with germ line *p16^{ink4}* mutations, loss of *p16^{ink4}* function may indeed be the initiating genetic event. In colon cancer where the genes involved in tumorigenesis are better characterized than in melanoma and more tumors have been analysed by microdissection, molecular data establish a preferred but not invariable order of genetic alterations

(Fearon and Vogelstein, 1990), which may also apply to the timing of $p16^{ink4}$ inactivation in melanoma.

In the analysed tumor, LOH at microsatellite D9S259 evolved independently of homozygous loss of $p16^{ink4}$. Our data thus support the assumption of other groups that, besides $p16^{ink4}$, at least one additional tumor suppressor gene involved in melanoma progression must exist on the short arm of chromosome 9 (Holland *et al*, 1994; Puig *et al*, 1995; Ohta *et al*, 1996; Morita *et al*, 1998; Wagner *et al*, 1998).

The $p16^{ink4}$-negative cell populations further harbor codeletions at DXS998 and D14S53. LOH on the X-chromosome in malignant melanoma has been previously reported (Dracopoli *et al*, 1987). It is believed to represent loss of the inactive and late replicating X, which would confer a proliferative advantage to the tumor cell due to shortening of the cell cycle. LOH at D14S53 independently arose in at least two tumor cell lineages as demonstrated by LOH affecting opposing alleles. The genealogic data underline the importance of this genetic change as it is unlikely that it occurred only by chance. Furthermore, LOH on the long arm of chromosome 14 is a common genetic alteration in ovarian carcinoma and two putative suppressor gene loci could be delineated: one at 14q12–13 and the other at 14q32 (Bandera *et al*, 1997). We cannot exclude the possibility that other structural mutations play a role in the progression of the analysed melanoma as the chosen microsatellite loci do not cover all chromosome arms and all known tumor suppressor genes.

The occurrence of codeletions supports the concept of tumor cell evolution through specific evolutionary pathways that are determined by the genetic burden of the tumor cells, i.e., the developmental limitations imposed by preceding genetic changes. This concept of evolutionary pathways may serve as an additional explanation for the observation that loss of $p16^{ink4}$ is strongly selected in some melanomas but not present in other cases. Further evidence for the existence of evolutionary pathways has been provided by a study demonstrating that, in primary melanomas, mutations of the $p16^{ink4}$ or $p15$ tumor suppressor genes do not occur concomitantly with microsatellite instability and vice versa, and thus may represent independent evolutionary pathways (Matsumura *et al*, 1998). Our data support this assumption to a certain extent as we could show that the cell lineage exhibiting abundant microsatellite instability suggestive of mismatch repair deficiency (Aquilina *et al*, 1994) did not harbor mutation or homozygous loss of $p16^{ink4}$. Nevertheless, we cannot rule out that $p16^{ink4}$ expression in this tumor cell population might have been inactivated by other mechanisms such as promotor methylation. On the other hand, two $p16^{ink4}$-negative tumor cell populations in the analysed melanoma (M2, M7) harbored microsatellite instability but at a significantly lower frequency compared to M6. It is not clear whether this observed microsatellite instability has the same genetic basis as the frequent replication errors detected in the cell population of metastasis M6 but it indicates that replication error and $p16^{ink4}$ inactivation may not invariably exclude each other.

Mutational pressure is one driving force of evolution that is counteracted by selective pressure. Epidemiologic studies of hereditary nonpolyposis colon cancer could show that this tumor type has a good prognosis despite the raised mutation rate caused by mismatch recognition deficiency. This indicates that the malignant potential of a tumor is not directly correlated to the degree of genetic instability (Tomlinson and Bodmer, 1999). The fate of the genetically unstable tumor cell population of metastasis M6 seems to support this view for melanoma as well. Although the cell lineage leading to M6 acquired more structural mutations than the $p16^{ink4}$-negative populations and was the first to form a visible lymph node metastasis, it does not appear to be clinically more malignant as the recurrent axillary metastases and the gastric metastasis originated from the $p16^{ink4}$-negative tumor cell populations which demonstrated less genetic instability. A second observation suggests a selective pressure against a raised mutation rate in the analysed malignant melanoma: the genealogic data show that very specific genetic alterations have occurred repeatedly and independently in the $p16^{ink4}$-negative tumor cell populations. As mutations, in general, mostly occur at random, one would expect a significant degree of random genetic alterations in a tumor cell population which has repeatedly acquired specific genetic changes. The lack of additional genetic alterations in the $p16^{ink4}$-negative tumor populations implies that most structural deletions have been eliminated by selection.

In summary, the evolutionary approach towards tumorigenesis and tumor progression used in this study confirms the role of $p16^{ink4}$ inactivation for melanoma progression but not for melanoma initiation in the case analysed. It also suggests the existence of additional putative tumor suppressor genes located on 9p as well as on the long arm of chromosome 14 and shows that microsatellite instability may represent an alternative pathway of tumor cell evolution in malignant melanoma. The analysed melanoma is characterized by a high degree of genetic heterogeneity within the primary tumor, which persists as independent tumor cell lineages in the metastases. Further studies will be necessary to decide whether multilineage progression is a frequent feature of malignant melanoma. The existence of multilineage progression in malignant melanoma would have profound implications for specific immunotherapy or gene therapy strategies as molecular analysis of one metastasis might not be representative of all tumor cell clones present in a patient.

The work was supported by grant PMT-A3 provided by the RWTH Aachen. We thank Prof. Dr. R. Osieka and Prof. H.F. Merk for their help in establishing an interdisciplinary cancer research group and Mrs. S. Isler for technical assistance.

REFERENCES

Aquilina G, Hess P, Branch P, MacGeoch C, Casciano I, Karran P, Bignami M: A mismatch recognition defect in colon carcinoma confers DNA microsatellite instability and a mutator phenotype. *Proc Natl Acad Sci USA* 91:8905–8909, 1994

Bandera CA, Takahashi H, Behbakht K, *et al*: Deletion mapping of two potential chromosome 14 tumor suppressor gene loci in ovarian carcinoma. *Cancer Res* 57:513–515, 1997

Bartkova J, Lukas J, Guldberg P, Alsner J, Kirkin AF, Zeuthen J, Bartek J: The *p16*-cyclin D/Cdk4-pRb pathway as a functional unit frequently altered in melanoma pathogenesis. *Cancer Res* 56:5475–5483, 1996

Boland CR, Sato J, Appelman HD, Bresalier RS, Feinberg AP: Microallelotyping defines the sequence and tempo of allelic losses at tumour suppressor gene loci during colorectal cancer progression. *Nat Med* 1:902–909, 1995

Boni R, Matt D, Voetmeyer A, Burg G, Zhuang Z: Chromosomal allele loss in primary cutaneous melanoma is heterogeneous and correlates with proliferation. *J Invest Dermatol* 110:215–217, 1998

Dracopoli NC, Alhadeff B, Houghton AN, Old LJ: Loss of heterozygosity at autosomal and X-linked loci during tumor progression in a patient with melanoma. *Cancer Res* 47:3995–4000, 1987

Fearon ER, Vogelstein B: A genetic model for colorectal tumorigenesis. *Cell* 61:759–767, 1990

Fujii H, Marsh C, Cairns P, Sidransky D, Gabrielson E: Genetic divergence in the clonal evolution of breast cancer. *Cancer Res* 56:1493–1497, 1996

Glendening JM, Flores JF, Walker GJ, Stone S, Albino AP, Fountain JW: Homozygous loss of the $p15^{ink4b}$ *gene (and not the* $p16^{ink4}$ gene) during tumor progression in a sporadic melanoma patient. *Cancer Res* 55:5531–5535, 1995

Goldstein AM, Tucker MA: Screening for CDKN2A mutations in hereditary melanoma. *J Natl Cancer Inst* 89:676–678, 1997

Healy E, Sikkink S, Rees JL: Infrequent Mutations of $p16^{ink4}$ in sporadic melanoma. *J Invest Dermatol* 107:318–321, 1996

Holland EA, Beaton SC, Edwards BG, Kefford RF, Mann GJ: Loss of heterozygosity and homozygous deletions on 9p21–22 in melanoma. *Oncogene* 9:1361–1356, 1994

Kamb A, Gruis NA, Weaver-Feldhaus J, *et al*: A cell cycle regulator potentially involved in genesis of many tumor types. *Science* 264:436–440, 1994

Lee JY, Dong SM, Shin MS, *et al*: Genetic alterations of $p16^{INK4a}$ and p53 genes in sporadic dysplastic nevus. *Biochem Biophys Res Commun* 237:667–672, 1997

Loeb LA, Christians FC: Multiple mutations in human cancers. *Mutat Res* 350:279–286, 1996

Matsumura Y, Nishigori C, Yagi T, Imamura S, Takebe H: Mutations of *p16* and p15 tumor suppressor genes and replication errors contribute independently to the pathogenesis of sporadic malignant melanoma. *Arch Dermatol Res* 290:175–180, 1998

Mirchandani D, Zheng J, Miller GJ, Gosh AK, Shibata DK, Cote RJ, Roy-Burman P: Heterogeneity in intratumor distribution of p53 mutations in human prostate cancer. *Am J Pathol* 147:92–101, 1995

Morita R, Fujimoto A, Hatta N, Takehara K, Takata M: Comparison of genetic profiles between primary melanomas and their metastases reveals genetic alterations and clonal evolution during progression. *J Invest Dermatol* 111:919–924, 1998

Nowell PC: The clonal evolution of tumor cell populations. *Science* 194:23–28, 1976

Ohta M, Berd D, Shimizu M, *et al*: Deletion mapping of chromosome region 9p21-p22 surrounding the CDKN2 locus in melanoma. *Int J Cancer* 65:762–767, 1996

Puig S, Ruiz A, Lázaro C, *et al*: Chromosome 9p deletions in cutaneous malignant melanoma tumors: the minimal deleted region involves markers outside the *p16* (CDKN2) gene. *Am J Hum Genet* 57:395–402, 1995

Reed JA, Loganzo F, Jr, Shea CR, *et al*: Loss of expression of the *p16*/cyclin-dependent kinase inhibitor 2 tumor suppressor gene in melanocytic lesions correlates with invasive stage of tumor progression. *Cancer Res* 55:2713–2718, 1995

Rübben A, Traidl C, Baron JM, Großendorf-Conen EI: Evaluation of non-radioactive temperature gradient single-strand conformation polymorphism analysis and of temperature gradient gel electrophoresis for the detection of HPV 6-variants in condylomata acuminata and Buschke–Loewenstein tumours. *Eur J Epidemiol* 11:501–506, 1995

Shibata D, Hawes D, Li ZH, Hernandez AM, Spruck CH, Nichols PW: Specific genetic analysis of microscopic tissue after selective ultraviolet radiation fractionation and the polymerase chain reaction. *Am J Pathol* 141:539–543, 1992

Shibata D, Schaeffer J, Li ZH, Capella G, Perucho M: Genetic heterogeneity of the c-K-ras locus in colorectal adenomas but not in adenocarcinomas. *J Natl Cancer Inst* 85:1058–1063, 1993

Talve L, Sauroja I, Collan Y, Punnonen K, Ekfors T: Loss of expression of the $p16^{INK4}$/CDKN2 gene in cutaneous malignant melanoma correlates with tumor cell proliferation and invasive stage. *Int J Cancer* 74:255–259, 1997

Tollenaar RA, Bonsing BA, Kuipers-Dijkshoorn NJ, Hermans J, van de Velde CJ, Cornelisse CJ, Fleuren GJ: Evidence of clonal divergence in colorectal carcinoma. *Cancer* 79:1304–1314, 1997

Tomlinson I, Bodmer W: Selection, the mutation rate and cancer: Ensuring that the tail does not wag the dog. *Nat Med* 5:11–12, 1999

Tsao JL, Tavare S, Salovaara R, Jass JR, Aaltonen LA, Shibata D: Colorectal adenoma and cancer divergence. Evidence of multilineage progression. *Am J Pathol* 154:1815–1824, 1999

Turbett GR, Barnett TC, Dillon EK, Sellner LN: Single-tube protocol for the extraction of DNA or RNA from paraffin-embedded tissue using a starch-based adhesive. *Biotechniques* 20:846–850, 1996

Wagner SN, Wagner C, Briedigkeit L, Goos M: Homozygous deletion of the $p16^{ink4a}$ and the $p15^{ink4b}$ tumour suppressor genes in a subset of human sporadic cutaneous malignant melanoma. *Br J Dermatol* 138:13–21, 1998

Walker GJ, Palmer JM, Walters MK, Hayward NK: A genetic model of melanoma tumorigenesis based on allelic losses. *Genes Chromosom Cancer* 12:134–141, 1995

Wiltshire RN, Duray P, Bittner ML, *et al*: Direct visualisation of the clonal progression of primary cutaneous melanoma: application of tissue microdissection and comparative genomic hybridisation. *Cancer Res* 55:3954–3957, 1995